Anomalous power dependence of sensitized upconversion luminescence

J. F. Suyver,* A. Aebischer, S. García-Revilla,† P. Gerner, and H. U. Güdel
Department of Chemistry and Biochemistry, University of Bern, Freiestrasse 3, 3000 Bern 9, Switzerland
(Received 5 November 2004; published 23 March 2005)

The expected excitation power dependencies for any upconversion emission band of an acceptor ion is investigated theoretically when the excitation takes place on a sensitizer ion and subsequent energy transfer upconversion from the sensitizer to the acceptor ion is exclusively responsible for the excitation of the acceptor ion. Under these limitations it is shown that emission from a state that requires k energy transfer upconversion steps will have a slope of k in the low-power regime when the luminescence intensity is plotted in a double-logarithmic representation versus absorbed pump intensity. In the high-power regime, any emission band will show a slope of 1, irrespective of the number of energy transfer steps from the sensitizer to the acceptor ions that are involved. The theoretical results are verified experimentally by data on three different inorganic systems with different types of sensitizer and acceptor ions: rare earth (RE) ions as well as transition metal (TM) ions. The active ions in the systems that are studied experimentally are RE/RE, RE/TM, and TM/TM, where the first dopant indicates the sensitizer ion and the second dopant indicates the upconverting ion. These different classes of sensitizer and upconverter ions all agree with the theoretical predictions put forward by the model. Thus providing confidence in the applicability (within the boundary conditions put forward here) of the model described.

DOI: 10.1103/PhysRevB.71.125123 PACS number(s): 78.20.−e, 42.65.Ky, 42.70.Nq, 78.55.−m

I. INTRODUCTION

In the field of optical spectroscopy special attention is given to nonlinear processes, such as second harmonic generation, photon upconversion, cooperative luminescence and so on. These processes have received a great deal of interest as they typically involve interesting physics due to the nontrivial power-dependence of the population densities of the excited states.[1] Since the theoretical prediction[2] and experimental observation[3,4] of near-infrared to visible photon upconversion via energy transfer processes, much research has been devoted to understanding the upconversion-induced luminescence characteristics.[1,5,6] Due to a large number of publications that indicated fascinating applications for upconversion phosphors, the field expanded rapidly.[7–11]

Initially, it was realized that the steady-state population density of a state (and therefore its associated luminescence intensity) scales with P^n, when n excitation photons are upconverted to excite emission from the state under investigation and the excitation power is given by P. As this power dependence could be checked experimentally, it was used as a direct measurement for the number of excitation photons involved in the excitation of the upconversion emission. However, when more powerful near-infrared excitation sources became available, it was noticed that at higher powers the P^n dependence began to reduce and finally even a "saturation" of the emission intensity could be observed, where increasing the excitation power no longer influenced the emission intensity at all.[12] Since no adequate explanation of this phenomenon existed, researchers continued to use power dependence of the emission intensity (in the low-power limit) as a measurement for the number of excitation photons involved in the excitation of the upconversion emission.

This experimentally observed saturation of the upconversion-induced luminescence with increasing excitation power was explained in 2000 when it was theoretically proven that the power-dependence of any upconversion emission band changes with excitation power.[13] Specifically, when an upconversion emission is excited by the sequential absorption and energy transfer upconversion of n photons, its dependence on absorbed pump power P decreases from P^n down to P^1 with increasing excitation power. However, this only applies for the highest energy electronic state that is excited through upconversion. Lower-lying states (excited by upconversion with m photons, where $m<n$) were predicted to have a power dependence that decreases from P^m down to $P^{(m/n)}$, which is even less than P^1, in the high-power limit. The publication included several experimental examples clearly demonstrating this effect in action.

The model, however, only included one type of ion responsible for the upconversion processes. Furthermore, the model exclusively assumed excited state absorption, or energy transfer upconversion from the lowest-lying excited state to higher states. Due to these boundary-conditions the applicability of the model is somewhat limited. The most significant omission is the group of materials where the excitation is initially absorbed on a sensitizer ion and then subsequently transferred to an acceptor ion that is responsible for the upconversion and emission. Typically, these materials are among the most efficient upconverters known, which is related to the fact that both the initial absorption on the sensitizer ion, and the energy transfer from the sensitizer to the acceptor ion can be very efficient. Oftentimes a sensitizer ion (typically Yb^{3+}) is purposely added to a specific material that already has an upconverting ion present in the host lattice (typically another trivalent rare earth ion) as this increases the upconversion efficiency. For such materials, where a sensitized photon upconversion process is dominant, the model described above cannot be applied.

In this paper, a model is presented that calculates the excitation power dependence of all population densities of an

upconverting acceptor ion that receives its energy via transfer from a sensitizer ion on which the energy was initially absorbed. The model requires only that the upconversion on the acceptor ion occurs through energy transfer from a sensitizer ion, but no further assumptions need to be imposed. Most notably, the energy transfer upconversion steps are not required to depend on the population density of a fixed state of the acceptor ion (such as the fixed dependence on the population of the first excited state in the model without a sensitizer). There is a large class of materials for which this assumption is expected to be valid. This fact will be demonstrated in the second part of the paper, where experimental data on three different upconverting materials will be presented. There it will be shown that the power dependence of the upconversion and downconversion emissions from the acceptor ions, as well as the excited state emission from the sensitizer ion itself, follow precisely the trend calculated by the model described in the next section.

II. MODEL

This section consists of two main parts. Section II A will describe and discuss for a simplified rate equation system the two limiting cases (i.e., the high- and low-power limits) that occur. The goal here is to understand the underlying trends in as simple a system as possible. Next, the general rate equation system will be presented in Sec. II B and the limiting cases of its solution will be investigated. Most importantly, it will be proven that in this general case identical high- and low-power limits can be obtained as were found for the simplified situation studied earlier.

Throughout this paper, two different types of ions will be considered: the sensitizer ions, and the acceptor ions. It will be assumed that the laser excitation will be exclusively absorbed on the sensitizer ions and subsequently (a fraction of) these excitations will be transferred to the acceptor ions. When P denotes the laser power and σ the excitation cross section for the sensitizer ions, then the steady state population of excited sensitizer ions, N_s, will be given by

$$N_s = \sigma P. \tag{1}$$

Note that this implies the assumption that the excitation cross section is independent of the laser power. This assumption is expected to be valid as long as no significant sample heating occurs as a result of the laser excitation. At very high laser powers, other power loss mechanisms such as second harmonic generation, color-center formation and sample destruction must be included. When these processes become dominant, the theory described here cannot be applied anymore.

A. Simplified model

For the simplified rate equation model, two important assumptions are made. These assumptions are graphically depicted in Fig. 1(a). First, it is assumed that exclusively emission transitions occur from state $|i\rangle$ of the acceptor ion directly to the ground state and that cross-relaxation processes and interexcited state emissions do not occur. Second,

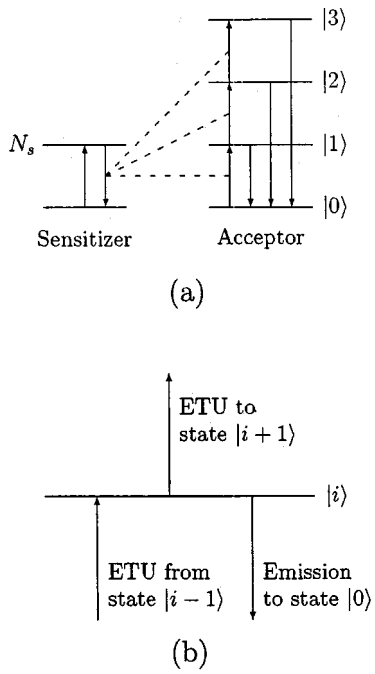

FIG. 1. Schematic representation of the energy transfer processes that can occur in the simplified model, as described in Sec. II A. Part (a) shows the processes relevant to the lowest lying states of the acceptor as well as those of the sensitizer ion. Part (b) shows the populating and depopulating processes for a general state $|i\rangle$ of the acceptor ion.

a perfect ladder of states on the acceptor ion is required. The energy separation between two adjacent states in this ladder is given by precisely the energy-gap from the ground state to the excited state of the sensitizer ion. As a result, for all states of the acceptor ion the energy transfer upconversion (ETU) step to the next higher-lying state will take place resonantly.

The model will describe the population of a general state $|i\rangle$ of the acceptor ion in terms of the processes and states that influence this state. Let N_i denote the steady state population density of the state $|i\rangle$, and N_s denote the (also steady state) excited state population density of the sensitizer ion. Furthermore, W_i will denote the upconversion rate constant associated with upconversion from state $|i\rangle$ to state $|i+1\rangle$ on the acceptor ion, and R_i is the relaxation rate constant from state $|i\rangle$ of the acceptor ion to the ground state. This total emission rate constant includes both nonradiative multiphonon relaxation as well as radiative emission.

Given these definitions, one can see that the the state $|1\rangle$ of the acceptor ion must be at the same energy as the excited state of the sensitizer ion. As a result of the energy transfer from the sensitizer ion to this state, it is found that in the steady state

$$N_1 \propto N_s. \tag{2}$$

Clearly, as also expected, this implies that the population of state $|1\rangle$ of the acceptor ion scales linearly with the laser power.

Under the assumptions described above, one can directly write down the balance equation for the steady state population density of state $|i\rangle$ of the acceptor ion,

$$W_{i-1}N_{i-1}N_s = (R_i + W_iN_s)N_i. \tag{3}$$

The processes represented by this equation are depicted graphically in Fig. 1(b), where one can directly see the physical relevance of each of the three terms in Eq. (3) for the acceptor ion: ETU from state $|i-1\rangle$ to state $|i\rangle$, emission to the ground state and ETU from state $|i\rangle$ to state $|i+1\rangle$.

From Eq. (3) the steady state population density of state $|i\rangle$ of the acceptor ion is found to be

$$N_i = \frac{W_{i-1}N_{i-1}N_s}{R_i + W_iN_s}. \tag{4}$$

The low- and high-power limits of this equation, and their associated solutions and underlying trends, will be discussed in the next two sections.

1. Low-power limit

In the low-power limit, upconversion from state $|i\rangle$ to state $|i+1\rangle$ can be ignored as relaxation to the ground state will be the dominant depopulation process. In other words, in the low-power limit the main depopulation process for the excited state is emission to the ground state, $R_i \gg W_iN_s$. Therefore, the balance equation for the population density of state $|i\rangle$ of the acceptor ion reduces from Eq. (3) to give

$$W_{i-1}N_{i-1}N_s = R_iN_i. \tag{5}$$

This equation has a trivial steady-state solution that is given by

$$N_i = \frac{N_{i-1}W_{i-1}N_s}{R_i}. \tag{6}$$

Thus, the population density of the state $|i\rangle$ will depend linearly on the population density of the state $|i-1\rangle$, multiplied by the population of the excited state of the sensitizer ion and a prefactor that is independent of the excitation power. Since one can write a similar relation for the population of the state $|i-1\rangle$ in terms of the population of the state state $|i-2\rangle$ multiplied by N_s, the final result becomes

$$N_i \propto (N_s)^i \propto P^i, \tag{7}$$

where P denotes the laser power. The last equivalence is due to Eq. (1). This well-known and intuitive result was already known for a long time[1] but had not yet been derived for sensitized energy transfer processes. It implies that in the low-power limit an emission band that requires i energy transfer upconversion steps to be excited will have exactly a slope of i when the luminescence intensity is plotted in a double-logarithmic representation versus absorbed pump power for a known pump focus (i.e., versus absorbed pump intensity). This result is identical to the low-power limit of the model determined for upconversion without a sensitizer.[13]

2. High-power limit

In the high-power limit, emission from state $|i\rangle$ to the ground state will be insignificant as upconversion to the state $|i+1\rangle$ will be the major depopulation process. In the terminology introduced above, this limit is reached when $W_iN_iN_s \gg R_iN_i$ and then the equation describing the population density of state $|i\rangle$ of the acceptor ion reduces from Eq. (3) to

$$W_{i-1}N_{i-1}N_s = W_iN_iN_s. \tag{8}$$

This equation has a straightforward steady-state solution that is independent of the excited state population of the sensitizer ion from which the energy transfer upconversion originates,

$$N_i = \frac{W_{i-1}}{W_i}N_{i-1} \propto N_{i-1}. \tag{9}$$

Note that from the fact that $N_i \propto N_{i-1}$, combined with Eqs. (1) and (2), this equivalence can be written as

$$N_i \propto N_s \propto P^1, \tag{10}$$

where P remains the laser power.

This result is clearly different from that obtained previously for energy transfer upconversion without sensitization,[13] by introducing the sensitizer ions, the resulting population density of state $|i\rangle$ of the acceptor ion will depend linearly on the population density of the state $|i-1\rangle$ and therefore the population densities of all energy levels of the acceptor ion must have the same power dependence in the high-power limit. Stated differently, in the high-power limit any emission band of the acceptor ion will have a slope of 1 when the luminescence intensity is plotted in a double-logarithmic representation versus pump power, regardless of the number of excitations and energy transfers involved.

3. Graphical overview

A schematic overview of the results obtained with this simplified model as compared to the model that describes energy transfer upconversion without a sensitizer is shown in Fig. 2. The population N_i of the three excited states $|i\rangle$ (where $i=1,2,3$) of an ion capable of energy transfer upconversion is shown as a function of the laser power. Note that the figures are plotted in a double-logarithmic representation and the ions capable of upconversion abide by the two assumptions of the simplified rate equation model, as described at the beginning of this section.

Figure 2(a) demonstrates the results obtained with the model briefly described in the Introduction.[13] There are three upconversion emission bands, which require the sequential absorption of 1, 2, and 3 photons to be excited, respectively. As a result, due to the double-logarithmic representation, the slopes shown in Fig. 2(a) in the low-power limit are 1, 2, and 3, respectively. In the high-power limit, the slope of 3 (the largest one) reduces to 1. The intermediate slopes reduce from 2 to 2/3 and from 1 to 1/3, respectively. This particular behavior has been demonstrated experimentally in several systems, such as for the four-step upconversion in $Cs_3Lu_2Cl_9:Er^{3+}$ under 6494 cm^{-1} excitation.[14]

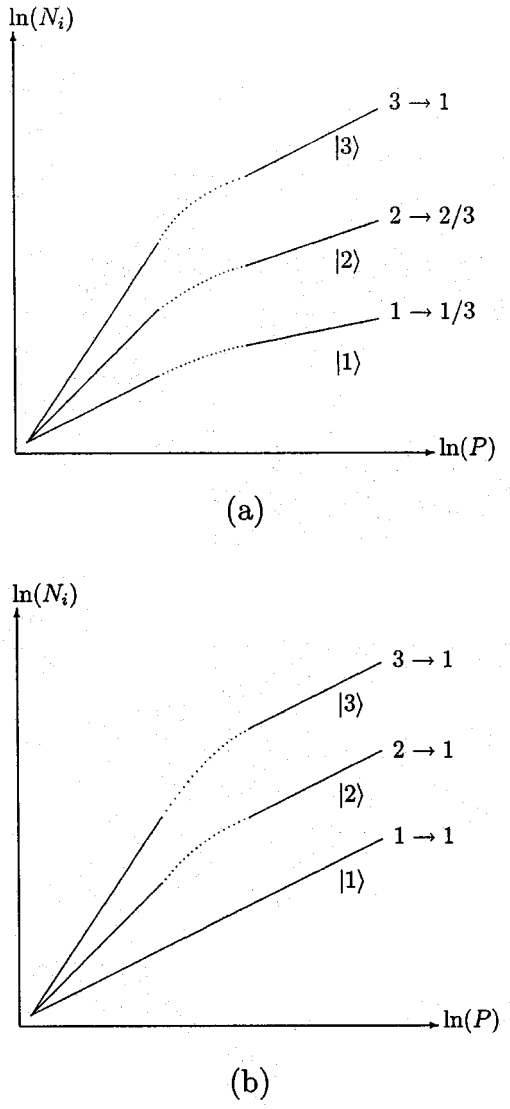

FIG. 2. Schematic representation of the population density of the three lowest-lying excited states $|i\rangle$ (where $i=1,2,3$) of an ion capable of energy transfer upconversion. Part (a) shows the expected trend derived in literature (Ref. 13) when only energy transfer upconversion on the acceptor ion is included (i.e., no sensitization). Part (b) shows the results from the model described in Sec. II A. For both graphs a double-logarithmic representation is used.

The different results obtained with the model described in this section are indicated clearly in Fig. 2(b). In the low-power limit the slopes are identical to those in Fig. 2(a) and are determined by the number of excitation photons that must be absorbed to observe emission from each of these bands. However, in the high-power limit calculations from the model indicate that all slopes must become parallel and are given by 1 in this range. After the discussion of the general case, several examples will be presented in Sec. III which will show this behavior experimentally.

Only the low- and high-power limits of Figs. 2(a) and 2(b) are simple predictions of the models. The intermediate (dotted) regions are not a straightforward prediction of either of the limiting cases of the models. To describe the precise form of this crossover region and its position on the $\ln(P)$ axis, one will need to use the full Eq. (4) and the result will depend on the microscopic materials parameters and the range of P used. As comparison, the experimental data will be based on the predictions of the low- and high-power limits only, the full Eq. (4) will not be used here.

B. General case

In the general case that is presented here, no assumptions are made regarding the energetic positions of specific states of the acceptor ion. As a result, the schematic representation shown in Fig. 1(a) can no longer be used since the equidistant energy level spacing does not apply here. Furthermore, in the general case interexcited state emissions are included as well. The only process not included in the general case is cross relaxation. This process is not treated as cases for which the main population or depopulation process for any of the electronic states is cross relaxation are rare. Furthermore, one would have to make additional assumptions regarding the values of the cross relaxation rate constants which would ensure a loss of generality of the model.

For the general case, N_i remains the steady state population density in the state $|i\rangle$ of the acceptor ion and N_s the excited-state population density of the sensitizer ion. The total emission rate constant from state $|i\rangle$ is denoted with R_i and the branching ratios from this state to the different states $|j\rangle$ $(j<i)$ will be given by η_{ij}. Again, this total emission rate includes both radiative emission as well as nonradiative multiphonon relaxation. The upconversion rate constant associated with upconversion from state $|i\rangle$ to state $|j\rangle$ on the acceptor ion is denoted as W_{ij}. When the energy difference between states $|i\rangle$ and $|j\rangle$ of the acceptor ion differs from the energy of the excited state of the sensitizer ion, no resonant energy transfer upconversion can take place and in this case the rate constant will be small. However, allowing for small (but nonzero) rate constants for phonon-assisted upconversion processes does not change the trends obtained from this model which therefore also includes phonon-assisted upconversion processes as long as the laser-induced heating of the sample (resulting in a change in the phonon-assisted upconversion rates) can be ignored. Naturally, due to the small rate constants involved with phonon-assisted upconversion, the laser powers required to experimentally observe the high-power limit will be much higher than for resonant energy transfer upconversion.

With these definitions, the full balance equation for the steady state population density in state $|i\rangle$ can be written as

$$\sum_{j<i} (W_{ji}N_jN_s - \eta_{ij}R_iN_i) = \sum_{j>i} (W_{ij}N_iN_s - \eta_{ji}R_jN_j). \quad (11)$$

Note that $\Sigma_{j<i}\eta_{ij}=1$ as the branching ratios are normalized to one. From this the steady state population density of state $|i\rangle$ can be derived analytically to be

$$N_i = \frac{\sum_{j>i} \eta_{ji}R_jN_j + \sum_{j<i} W_{ji}N_jN_s}{R_i + \sum_{j>i} W_{ij}N_s}. \quad (12)$$

The limiting cases of the population density obtained in Eq. (12) will be discussed in the following sections. Note

that the slope of the luminescence intensity of the sensitizer ion, when double-logarithmically plotted versus pump power used, will remain one and will not depend on the excitation power as can be seen from Eq. (1).

Finally, it should be mentioned again that the theory described here assumes that no sample heating takes place. In a physical system, the high-power limit can be associated with heating of the sample which leads to changes in the absorption cross section. As a result, a deviation from a linear increase of the sensitizer population with pump-power will occur at the highest excitation powers and in this regime the model can no longer be applied.

1. Low-power limit

The low-power limit of Eq. (12) will be reached when the sensitizer-related energy transfer upconversion term for state $|i\rangle$ is insignificant compared to the term relating to emission of the acceptor ion,

$$\sum_{j>i} W_{ij} N_i N_s \ll \sum_{j<i} \eta_{ij} R_i N_i. \tag{13}$$

The population of the state occurs through energy transfer from the sensitizer ion, while the depopulation occurs through relaxation to all lower-lying states of the acceptor ion. This results in a power-dependence for the low-power limit that is found by incorporating Eq. (13) into Eq. (11), resulting in

$$N_i = \sum_{j<i} \frac{W_{ji} N_j}{R_i} N_s. \tag{14}$$

From Eq. (14) it can be seen that the population of state $|i\rangle$ will scale with the excited-state population density of the sensitizer ion multiplied by the population density of the state from which the upconversion on the acceptor ion originated. Similarly to that shown in Sec. II A 1, this implies that, in the low-power limit, when k energy transfer upconversion steps are required to reach state $|i\rangle$, the power-dependent population density of this state will scale with

$$N_i(k \times \mathrm{ETU}) \propto (N_s)^k \propto P^k. \tag{15}$$

From Eq. (14) it is clear that the general rate equation result reproduces the same trend in the low-power limit as was observed many times, both theoretically as well as experimentally for many different materials, a k-photon process will have a slope of k when the luminescence intensity is double-logarithmically plotted versus pump power used.[1,6,13]

2. High-power limit

From Eq. (11) it can be seen that for any state $|i\rangle$ the high-power limit will be reached when the term related to upconversion to any other state is dominant compared to the emission to the lower-lying states. This is described by the requirement that

$$\sum_{j<i} \eta_{ij} R_i N_i \ll \sum_{j>i} W_{ij} N_i N_s. \tag{16}$$

From this condition it is found that Eq. (12) reduces to

$$N_i = \frac{\sum_{j<i} W_{ji} N_j}{\sum_{j>i} W_{ij}} \propto \sum_{j<i} N_j. \tag{17}$$

The direct consequence of Eq. (17) is that the population density of any state $|i\rangle$ will scale linearly with the weighted sum of the populations of all the states $|j\rangle$ (where $j<i$). One can similarly write the population of state $|i-1\rangle$ in terms of a weighted sum of the populations of all the states $|j\rangle$ (where $j<i-1$). Therefore, in the high-power limit all populations densities must converge to the same laser power dependence: they will become linearly dependent on the population density of the excited state of the sensitizer ion (i.e., on the excitation power),

$$N_i(k \times \mathrm{ETU}) \propto N_s \propto P^1. \tag{18}$$

The last equivalence is due to Eq. (1) and this result is similar to what was seen before in the simplified model presented in Sec. II A 2.

When $|i\rangle$ would be the highest-energy state and no further upconversion is possible from this state, the result for this highest-energy state will be different. In such a case the population would scale with the population of the state feeding it multiplied by N_s. As a result of Eqs. (18) and (1), a power dependence of P^2 will be found in this case. The results for all lower-lying states would still abide by Eq. (18). No experimental examples of this effect have been found, as typically many states or even a broad-band continuum are found at high energy.

III. EXPERIMENTAL EXAMPLES

Three different examples have been chosen to provide experimental evidence for the validity of the model described. As the required high-power limits are only obtained when upconversion becomes a significant depopulation mechanism, reasonably efficient upconversion materials will be described. The three examples furthermore represent the three markedly different classes of sensitized upconversion known, rare-earth/rare-earth, rare-earth/transition metal, and transition metal/transition metal (denoted as sensitizer ion/upconverter ion). For these examples, the dominant upconversion mechanisms have been investigated in detail, and a proof of the sensitized nature of the energy transfer upconversion has been found for each system.[15–19] The samples under investigation were synthesized in house[18–20] and the relevant power-dependent emission data have not been published in the literature previously.

The materials were excited with a multimode, standing wave Ti:sapphire laser (Spectra Physics 3900S), pumped by an argon-ion laser in all-lines mode (Spectra Physics 204515/4S) or the second harmonic of a $Nd:YVO_4$ laser (Spectra Physics Millennia CS-FRU). The wavelength control of the Ti:sapphire laser was achieved by an inchworm driven (Burleigh PZ-501) birefringent filter and a wave meter (Burleigh WA2100). Sample cooling was achieved using a quartz helium gas flow tube. The sample luminescence was dispersed by a 0.85 m double monochromator (Spex 1402) with gratings blazed at 500 nm (1200 grooves/mm). The signal was

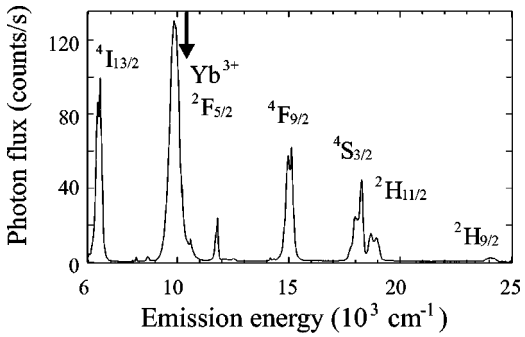

FIG. 3. Emission spectrum of the $NaYF_4$: 18% Yb^{3+}, 2% Er^{3+} sample. The excitation energy (indicated by the arrow) was at 10 238 cm^{-1}. The measurement was recorded at room temperature and in the high-power limit (~60 W/cm^2, unfocussed). The Yb^{3+} emission at 10 000 cm^{-1} and the emitting states of Er^{3+} are labeled in the figure.

detected with a cooled photomultiplier tube (Hamamatsu R3310) and a photon counting system (Stanford Research SR400). Device control and data acquisition were done by a personal computer. The luminescence spectra were corrected for the instrument response and the refractive index of air. The spectra are displayed as a photon flux per constant energy interval.[21] To measure the power dependence, the beam was attenuated with a series of neutral density filters (Balzers). The laser power was measured with a Coherent LabMaster power meter equipped with an LM10 power head. For the Cs_2NaYCl_6, 2% V^{3+}, 2% Re^{4+}; and for $CsCdBr_3$, 0.3% Yb^{3+}, 3.8% Ni^{2+} samples, the excitation laser was focused with a lens of $f=53$ mm and the corresponding laser power density was calculated as $P\pi w_0^2\lambda^{-2}f^{-2}$, where P is the laser power, w_0 the radius of the unfocussed laser beam, λ the excitation wavelength, and f the focal length of the lens.[22]

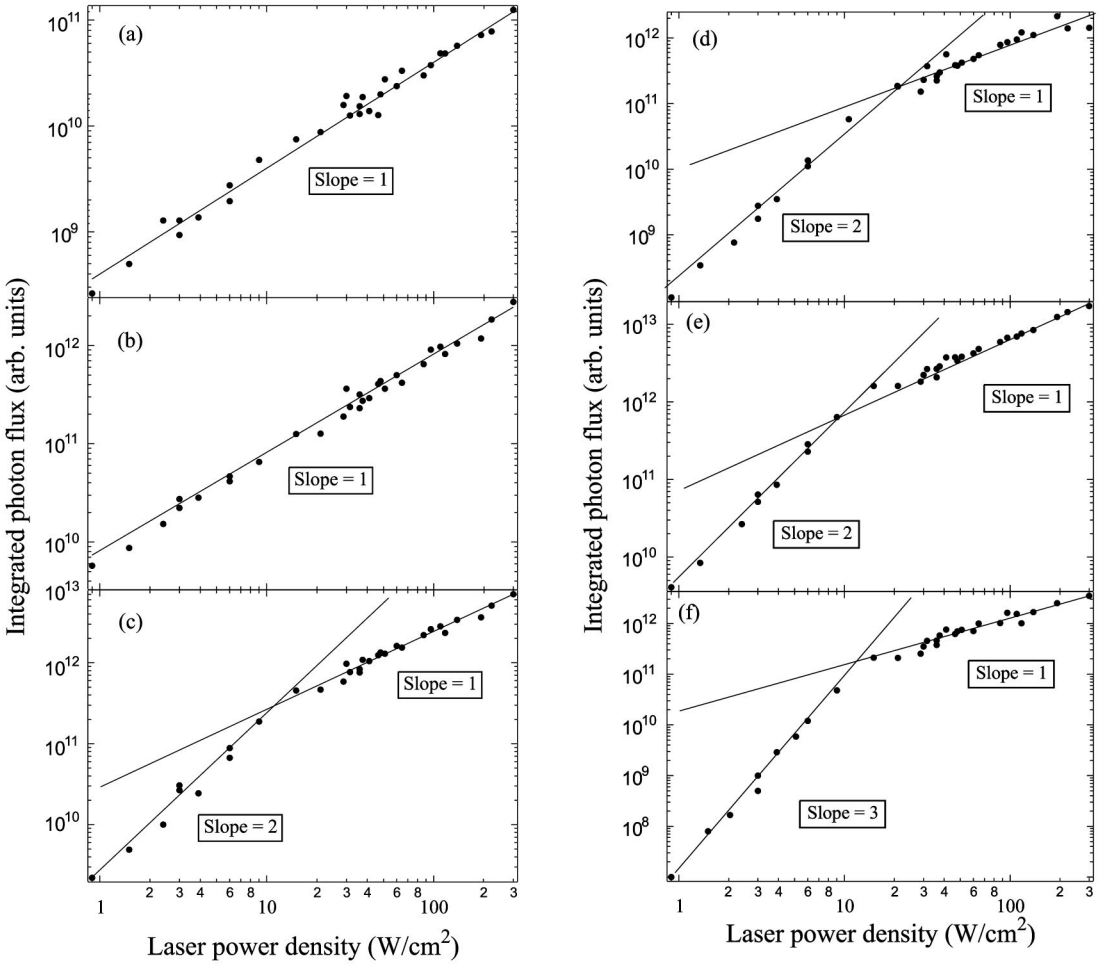

FIG. 4. Excitation power dependence of the following transitions of the $NaYF_4$: 18% Yb^{3+}, 2% Er^{3+} sample, (a) $^4I_{13/2}\rightarrow{}^4I_{15/2}$ at 6500 cm^{-1}, (b) $^2F_{5/2}\rightarrow{}^2F_{7/2}$ and $^4I_{11/2}\rightarrow{}^4I_{15/2}$ at 10 000 cm^{-1}, (c) $^4S_{3/2}\rightarrow{}^4I_{13/2}$ at 11 800 cm^{-1}, (d) $^4F_{9/2}\rightarrow{}^4I_{15/2}$ at 15 000 cm^{-1}, (e) $^4S_{3/2}\rightarrow{}^4I_{15/2}$ at 18 200 cm^{-1}, and (f) $^2H_{9/2}\rightarrow{}^4I_{15/2}$ at 24 000 cm^{-1}. The data was recorded at room temperature, excitation was at 10 238 cm^{-1} (indicated by the arrow in Fig. 3) and each emission band was integrated. Similar results were obtained under 10 200 cm^{-1} excitation (into a Yb^{3+} crystal field level relatively far away from any Er^{3+} absorption lines). The vertical scales cannot be compared. Note the logarithmic axes. The lines represent the calculations from the model in the high- and low-power limits according to Eqs. (18) and (14), respectively. The line in part (b) is given by Eq. (1).

A. $NaYF_4$: 18% Yb^{3+}, 2% Er^{3+}

Figure 3 shows the room temperature emission spectrum of $NaYF_4$: 18% Yb^{3+}, 2% Er^{3+}, one of the most efficient near-infrared to visible upconversion materials known. Under 10 238 cm^{-1} excitation, nearly all excitation photons are absorbed on the Yb^{3+} and in the high power-limit at least 65% of these are subsequently transferred to Er^{3+} where about 50% of the excitation photons contribute to the three visible upconversion emissions.[16] With the exception of the 10 000 cm^{-1} emission (mainly due to the Yb^{3+} sensitizer transition $^2F_{5/2} \rightarrow {}^2F_{7/2}$), all emission bands observed are related to intra-$4f$ transitions of the Er^{3+} acceptor ion. Their assignments are indicated in Fig. 3, as well as in the caption of Fig. 4.

Figure 4 shows the integrated photon flux of each of the six major emission bands as a function of the laser power density. The lines through the data are the calculations from the model for the low- and high-power limits. Note that these lines do not include any fitting parameters other than a vertical scaling factor, and their slopes at low power are simply determined by the number of excitation photons required to excite any emission band, and by a slope of 1 in the high-power limit, as given by Eqs. (14) and (18), respectively.

It is clear from the lines in Figs. 4(a)–4(f) that the model describes the experimental data very well for all emission bands. Furthermore, it is also clear that the power density required to observe a crossover in the upconversion emission intensities (from a slope larger than 1, to a slope of 1), is different for the different emission bands. This fact proves that this crossover cannot be related to sample-heating in the high-power limit. Therefore, it must be attributed to an excitation power induced change in the net excited-state dynamics. This results in a change of the dominant depopulation process for the specific excited state under investigation. The actual power density for the crossover point from the low- to the high-power behavior is determined by a complex interplay between the relevant energy transfer processes, upconversion, cross-relaxation, radiative and nonradiative decay. Since in this regime there are a great number of possible fitting parameters (all the W_{ij} and η_{ij}) which influence the theoretical curve given by Eq. (12), no attempt has been made to model the power-dependence of the emission intensity near the crossover point.

B. $CsCdBr_3$: 0.3% Yb^{3+}, 3.8% Ni^{2+}

Figure 5 shows the low temperature (12 K) emission spectrum of $CsCdBr_3$: 0.3% Yb^{3+}, 3.8% Ni^{2+} under 10 604 cm^{-1} excitation (indicated by the arrow). A lens was used to reach the high-power limit. The excitation energy is chosen such that exclusively excitation into the Yb^{3+} $^2F_{5/2}$ occurs. As a result of this excitation energy, three main emission bands are observed. Two of these are related to the Yb^{3+} sensitizer ion, the direct Yb^{3+} emission at 9960 cm^{-1} and the cooperative Yb^{3+} pair-emission[23] at 19 570 cm^{-1}. The Ni^{2+} related $^1T_{2g} \rightarrow {}^3A_{2g}$ emission is observed at 14 350 cm^{-1}. This emission is related to a two-photon upconversion process[19] whereby the Ni^{2+} first receives an energy transfer from the Yb^{3+} $^2F_{5/2}$ state to populate the metastable Ni^{2+} $^3T_{2g}$

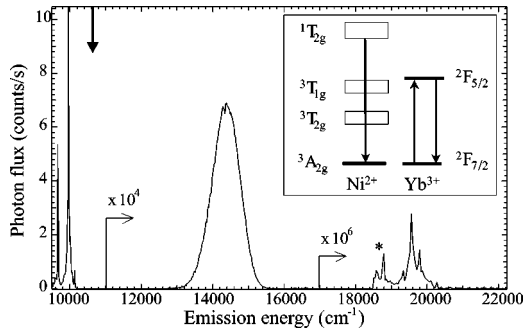

FIG. 5. Emission spectrum of the $CsCdBr_3$: 0.3% Yb^{3+}, 3.8% Ni^{2+} sample. The excitation energy (indicated by the arrow) was at 10 604 cm^{-1} and the measurement was recorded at 12 K and in the high-power limit ($\sim$5 kW/cm^2, focused). Note the two distinctly different vertical scaling factors for the upconversion emission part of the spectrum. The double-peak indicated by the asterisk at 18 700 cm^{-1} is due to some stray light from the green pump-laser for the Ti:saphire laser and its intensity is independent of the attenuation of the infrared laser intensity. The inset shows the relevant Yb^{3+} and Ni^{2+} energy levels as well as the excitation (upward arrow) and emissions (downward arrows) that are observed in this sample.

state, which subsequently serves as the initial state for another Yb^{3+} $^2F_{5/2}$ energy transfer to be excited into the $^1T_{2g}$ state of Ni^{2+} from which the upconversion emission is observed.

Figure 6 shows the laser power dependence of the three integrated emission bands in $CsCdBr_3$: 0.3% Yb^{3+}, 3.8% Ni^{2+}. From Fig. 6(a) it is clear that the Yb^{3+} (sensitizer) emission has a slope of 1 for all excitation densities used, in agreement with Eq. (1). In contrast [see Fig. 6(b)], the Ni^{2+} upconversion emission begins with a slope of 2 and for larger excitation densities gradually reduces to 1. This effect is well reproduced by the model, as can be seen from the lines through the data. From Fig. 6(c) it can be seen clearly that the Yb^{3+} cooperative pair-emission retains its slope of 2, regardless of the power density. Even though the excitation of this emission is a two-photon process, as is the case for the Ni^{2+} emission from the $^1T_{2g}$ state, a decrease of the slope is not expected for this Yb^{3+} cooperative pair-emission. The reason is that for the Yb^{3+} pair-emission no energy transfer steps are involved in the cooperative upconversion process. The fact that the Ni^{2+} upconversion emission starts out with a slope of 2, but reaches a slope of 1 in the high-power limit, while the Yb^{3+} pair-emission retains its slope of 2 is a very nice illustration of the applicability of the model presented in the preceding section and excludes possible experimental errors.

C. Cs_2NaYCl_6: 2% V^{3+}, 2% Re^{4+}

Figure 7 shows the room temperature emission spectrum of a Cs_2NaYCl_6: 2% V^{3+}, 2% Re^{4+} sample under 11 350 cm^{-1} excitation in the high-power limit (again, a lens was used to reach this limit). This excitation is into the $^3T_{2g}$ absorption band of V^{3+}, which acts as a sensitizer in this system. The energy level scheme is indicated in the inset of

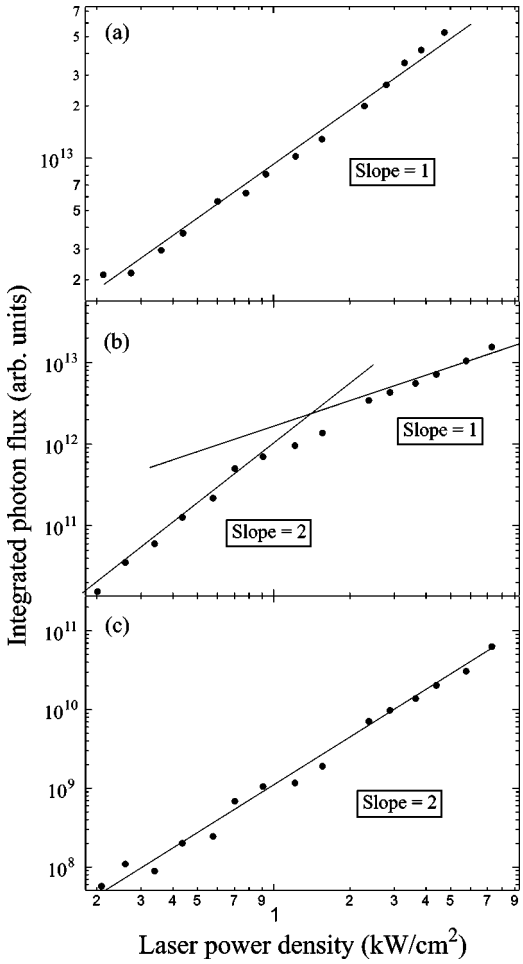

FIG. 6. Excitation power dependence at 12 K of the following transitions for the $CsCdBr_3$: 0.3% Yb^{3+}, 3.8% Ni^{2+} sample, (a) Yb^{3+} $^2F_{5/2}\rightarrow{}^2F_{7/2}$ at 9960 cm^{-1}, (b) Ni^{2+} $^1T_{2g}\rightarrow{}^3A_{2g}$ at 14 350 cm^{-1}, and (c) Yb^{3+} pair-emission at 19 570 cm^{-1}. The vertical scales cannot be compared. The sample was excited at 10 604 cm^{-1} (indicated by the arrow in Fig. 5) and the emission bands were integrated. Note the logarithmic axes. The line in part (a) is given by Eq. (1). The lines in part (b) represent the calculated power dependencies in the high- and low-power limits according to Eqs. (18) and (14), respectively. The line in part (c) has a slope of 2 and is discussed in the text.

Fig. 7. Two emissions are observed and they are assigned as the V^{3+} $^1T_{2g}\rightarrow{}^3T_{2g}$ transition (at 8500 cm^{-1}) and the Re^{4+} $\Gamma_7(^2T_{2g})\rightarrow\Gamma_8(^4A_{2g})$ transition (centered at 13 800 cm^{-1}).[18]

Figure 8 shows the influence of the laser power density on the sensitizer and acceptor emissions in Cs_2NaYCl_6: 2% V^{3+}, 2% Re^{4+}. Clearly, the V^{3+} (sensitizer) emission retains a slope of one irrespective of the power density, in accordance with Eq. (1). The Re^{4+} (acceptor) emission, on the other hand, has a slope of 2 in the low-power regime which gradually reduces to a slope of 1 in the high-power limit, which agrees well with the calculations from the model as given by Eqs. (14) and (18). For much higher excitation densities, small deviations from a slope of 1 are observed in the data, resulting in a slope less than 1 in this limit (not shown). This effect is attributed to the reduced excitation cross section of

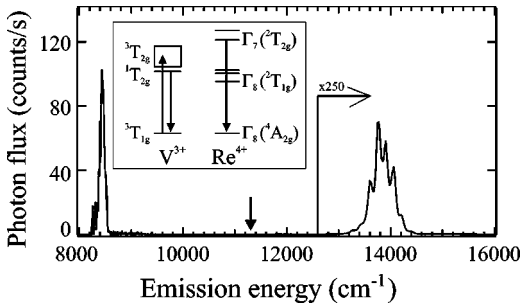

FIG. 7. Emission spectrum of the Cs_2NaYCl_6: 2% V^{3+}, 2% Re^{4+} sample. The excitation energy (indicated by the arrow) was at 11 350 cm^{-1} and the measurement was recorded at room temperature and in the high-power limit (~25 kW/cm^2, focused). Note the vertical scaling for the upconversion emission part of the spectrum. The inset shows the relevant V^{3+} and Re^{4+} energy levels as well as the excitation (upward arrow) and emissions (downward arrows) that are observed in this sample.

V^{3+} due to sample heating. The data below 30 kW/cm^2, as shown in the figure, are in good agreement with the model.

IV. CONCLUSIONS

In this paper the influence of the excitation power on the upconversion emission intensity is shown theoretically as well as experimentally in the case where the excitation oc-

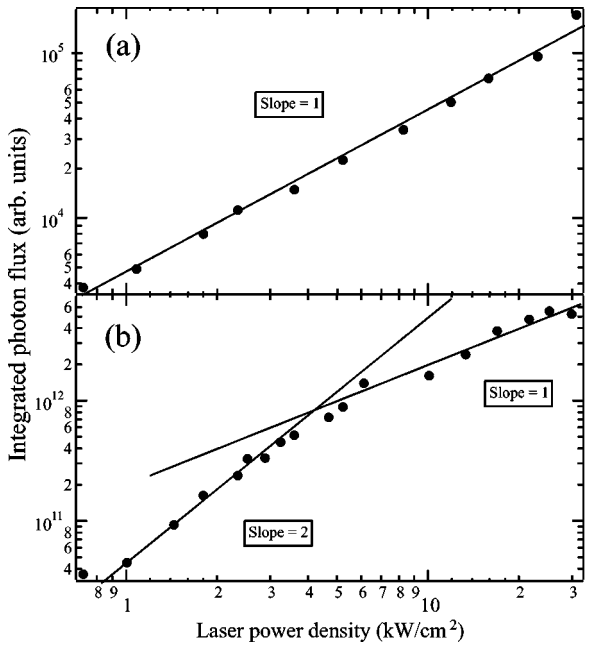

FIG. 8. Laser power dependence of the integral of the following transitions in the Cs_2NaYCl_6: 2% V^{3+}, 2% Re^{4+} sample, (a) V^{3+} $^1T_{2g}\rightarrow{}^3T_{1g}$ at 8500 cm^{-1} and (b) Re^{4+} $\Gamma_7(^2T_{2g})\rightarrow\Gamma_8(^4A_{2g})$ at 13 800 cm^{-1}. The excitation energy was at 11 350 cm^{-1} (indicated by the arrow in Fig. 7) and the measurement was performed at room temperature. The vertical scales of (a) and (b) cannot be compared. The line in part (a) is given by Eq. (1). The lines in part (b) represent the calculated power dependencies in the low- and high-power limits according to Eqs. (14) and (18), respectively.

curs on a sensitizer ion and is subsequently transferred to an acceptor ion. From the theory it is clear that in the low-power limit, the power-dependence of the upconversion emission from a state that requires n energy transfer upconversion steps will be given by P^n, where P denotes the excitation power. In the high-power limit, the power-dependence reduces to P^1, regardless of the actual number of energy transfer upconversion steps involved in the excitation process of the emitting state of the acceptor ion. The experimental examples provided ($NaYF_4$: 18% Yb^{3+}, 2% Er^{3+}; $CsCdBr_3$: 0.3% Yb^{3+}, 3.8% Ni^{2+}; and Cs_2NaYCl_6: 2% V^{3+}, 2% Re^{4+}; where the the sensitizer and upconverter ions are indicated as first and second dopants, respectively) show that this effect occurs whenever a sensitized energy transfer upconversion process is responsible for populating the emitting state of the acceptor ion. As the examples deal with very different classes of sensitizer and upconverter ions (i.e., both rare earth ions as well as transition metal ions), it is expected that the model can be applied generally whenever the upconversion emission is excited via a sensitizer ion. Therefore, the characteristic power-dependence fingerprint presented here can be used as a proof for the sensitized nature of the upconversion emission.

ACKNOWLEDGMENTS

Marieke van Veen is gratefully acknowledged for a careful reading of the paper. Markus Pollnau (Lausanne, Switzerland) is acknowledged for stimulating discussion. Daniel Biner is acknowledged for synthesizing the $NaYF_4$, 18% Yb^{3+}, 2% Er^{3+} sample. This work was financially supported by the Swiss National Science Foundation.

*Present address: Philips Research Laboratories, Eindhoven, The Netherlands. Electronic address: suyver@iac.unibe.ch

†Present address: Department of Applied Physics, University of Cantabria, Spain.

[1] F. Auzel, Chem. Rev. (Washington, D.C.) **104**, 139 (2004) and references therein.

[2] N. Bloembergen, Phys. Rev. Lett. **2**, 84 (1959).

[3] V. V. Ovsyankin and P. P. Feofilow, JETP Lett. **3**, 322 (1966).

[4] F. Auzel, Proc. IEEE **61**, 758 (1973) and references therein.

[5] G. Huber, E. Heumann, T. Sandrok, and K. Petermann, J. Lumin. **72/74**, 1 (1997).

[6] D. R. Gamelin and H. U. Güdel, Top. Curr. Chem. **214**, 1 (2001) and references therein.

[7] N. Menyuk, K. Dwight, and J. W. Pierce, Appl. Phys. Lett. **21**, 159 (1972).

[8] J. S. Chivian, W. E. Case, and D. D. Eden, Appl. Phys. Lett. **35**, 124 (1979).

[9] E. Downing, L. Hesselink, J. Ralston, and R. Macfarlane, Science **273**, 1185 (1996).

[10] M. F. Joubert, Opt. Mater. (Amsterdam, Neth.) **11**, 181 (1999).

[11] J. F. Suyver, A. Aebischer, D. Biner, P. Gerner, J. Grimm, S. Heer, K. Krämer, C. Reinhard, and H. U. Güdel, Opt. Mater. (Amsterdam, Neth.) (to be published).

[12] S. Singh and J. E. Geusic, Phys. Rev. Lett. **17**, 865 (1966).

[13] M. Pollnau, D. R. Gamelin, S. R. Lüthi, H. U. Güdel, and M. P. Hehlen, Phys. Rev. B **61**, 3337 (2000).

[14] S. R. Lüthi, M. Pollnau, H. U. Güdel, and M. P. Hehlen, Phys. Rev. B **60**, 162 (1999).

[15] A. Bril, J. L. Sommerdijk, and A. W. de Jager, J. Electrochem. Soc. **122**, 660 (1975).

[16] J. F. Suyver, J. Grimm, K. W. Krämer, and H. U. Güdel, J. Lumin. (to be published).

[17] A. Aebischer and H. U. Güdel, J. Alloys Compd. **374**, 60 (2004).

[18] A. Aebischer, O. S. Wenger, and H. U. Güdel, J. Lumin. **102–103**, 48 (2003).

[19] S. García-Revilla, P. Gerner, O. S. Wenger, H. U. Güdel, and R. Valiente, Chem. Phys. Lett. **401**, 492 (2005).

[20] K. W. Krämer, D. Biner, G. Frei, H. U. Güdel, M. P. Hehlen, and S. R. Lüthi, Chem. Mater. **16**, 1244 (2004).

[21] E. Edjer, J. Opt. Soc. Am. **59**, 223 (1969).

[22] A. E. Siegman, *Lasers* (University Science Books, Sausalito, 1986).

[23] E. Nakazawa and S. Shionoya, Phys. Rev. Lett. **25**, 1710 (1970).